

Spring 5-1-2006

## **Preparation and Purification of Enlarged Multinucleated U937 Human Leukemia Cells and their Susceptibility to Physical Damage by Ultrasound**

Kathryn Gold

Follow this and additional works at: [https://surface.syr.edu/honors\\_capstone](https://surface.syr.edu/honors_capstone)



Part of the **Biology Commons**

---

### **Recommended Citation**

Gold, Kathryn, "Preparation and Purification of Enlarged Multinucleated U937 Human Leukemia Cells and their Susceptibility to Physical Damage by Ultrasound" (2006). *Syracuse University Honors Program Capstone Projects*. 640.

[https://surface.syr.edu/honors\\_capstone/640](https://surface.syr.edu/honors_capstone/640)

## INTRODUCTION

### *Cancer and the neoplastic cell*

Cancer is a class of diseases characterized by the pathological generation of abnormal cells. The cancer begins as a localized growth that may spread throughout the body by the circulatory and lymphatic pathways. The poorly regulated cell division is caused by damage to the DNA and to mutations in genes that control cell division. Several mutations are required to turn a cell completely neoplastic, meaning that the transition from a normal cell to a cancerous (neoplastic) one can be a gradual process sometimes requiring years. Thus, each cancer is the end result of multiple changes within a single cell lineage that have taken place during the life of the affected cell or even within the germ line of the host. The critical biological changes within the cell that accompany its neoplastic transformation involve an altered response to mechanisms that control cell growth, differentiation, and senescence. Although there are many types of cancer, depending on the cell type of origin (connective tissue, hematopoietic tissue, or epithelial tissue), each grows and spreads in its own way and causes its own set of symptoms.

Cancer cells have many key behaviors that differentiate them from normal cells. One characteristic of the neoplastic cell is a reduced dependence on signals from other cells for its growth, survival, and division. Often, this is because they contain mutations in components of the cell signaling pathways through which the cells respond to such social cues. Neoplastic cells also have prolonged survival rates and are less prone to kill themselves by apoptosis than non-cancerous cells.

This aversion to suicide is often caused by mutations in genes that regulate the intracellular death program. A third characteristic of neoplastic cells is their ability to proliferate indefinitely. Most normal human somatic cells will divide only a limited number of times in culture, after which they permanently stop because the telomeres on the ends of the chromosomes become too short. Cancer cells typically break through this barrier by reactivating production of the telomerase enzyme that maintains telomere length.

In addition, neoplastic cells are often genetically unstable, because they have a greatly increased mutation rate and often have an impaired ability to repair damaged DNA. They can become invasive by changes in cell-adhesion molecules that hold normal cells in their proper place, by generating enzymes that allow them to invade through tissues, and by acquiring the ability to move. Lastly, cancer cells can often survive and proliferate in secondary tissues to form metastases, whereas most normal cells do not migrate from their original position to other sites in the organism.

Once cells have converted into the neoplastic phenotype, they can become invasive and often even metastatic. This invasive property allows them to penetrate their surrounding normal tissue barriers and move to a new location within the body, producing secondary tumors. This establishment of secondary tumors in the body is known as metastasis and proceeds through a clearly defined cascade of events. The first step of the cascade is the enzymatic digestion of the basement membrane, which allows the cell access to connective tissue and an avenue to detach from the primary tumor (McKinnell et al., 1998). The ability of a cell to detach and move is a fundamental property that malignant cancer cells exhibit. After the cells detach from the primary tumor, they have the ability to

move and invade a secondary location. The invasion of the cell into an adjacent tissue depends on the motility of the cell. Cancer cells can disseminate via capillary and lymphatic vessels (McKinnell et al., 1998). Once inside the capillaries, the cancer cells have the ability to adhere to one another, as well as to lymphocytes and platelets, forming emboli that can be stabilized by fibrin clotting (McKinnell et al., 1998). The circulating cancer cells can arrest at a secondary location and grow at that site completing the dissemination of malignant cells. Metastasis of cancer accounts for much of its lethality. Interruption of any of the steps of the cascade has the potential to disrupt the malignant spread and limit the malignant pathology. In cancer, because cell production is not balanced with cell loss, the cell population increases in number. Genetic instability leads to the generation of diverse cell variants, some of which may be able to metastasize to new locations. The lungs and the liver are the two most common sites for metastasis in the human body. Once in a new site, a cell must again penetrate the basement membrane of the blood vessel and establish itself in the new tissue, for its own growth and survival.

### *The Cell Cycle and its Regulation*

The cell cycle is a sequence of duplication and division of the cell. The function of the cycle is to duplicate DNA in the chromosomes and then precisely distribute the copies into genetically identical daughter cells. The cell cycle includes the manufacturing of DNA synthesis enzymes, the doubling of DNA, the synthesis of mitosis proteins, and then mitosis--the cell division. The period between one M phase (mitosis and cytokinesis) and the next M phase is called

interphase. Interphase is divided into the remaining three phases of the cell cycle. The cycle begins with G<sub>1</sub> and ends each round with a doubling of the cell. The G<sub>1</sub> phase is the first of the four stages of the cell cycle in which new organelles are synthesized and DNA synthesis enzymes are manufactured. This phase is remarkably longer than other phases because the daughter cells remain in G<sub>1</sub> until they receive a stimulus to enter the S phase (Alberts et al., 2004). The S phase is the synthesis stage in which nuclear DNA is replicated. At the end of this stage, the cell contains two complete sets of DNA. The G<sub>2</sub> phase follows the S phase and is a relatively short, pre-mitotic phase. Through internal biochemical changes, RNA and other specialized proteins are produced that will aid in the process of mitosis. The M phase is the final stage of the cell cycle and is a continuous process of cell division. However, it can be divided into four sub-phases that are marked by unique events.

The first event of mitosis occurs in prophase, in which the chromatin is transformed into chromosomes, with each chromosome composed of a pair of filaments called chromatids (Alberts et al., 2004). Also during prophase, the nuclear membrane disappears. During metaphase, the second phase of mitosis, the chromosomes align between the centrioles at the equatorial plate. They are positioned in such a way that when the chromatids separate, each daughter cell will have a complete set of chromosomes. Anaphase, the third phase, is marked by the separation of the sister chromatids and the formation of two daughter chromosomes, in which each chromosome is pulled toward the pole that it faces. The contractile ring also assembles during anaphase. During the final stage of mitosis, telophase, the two sets of daughter chromosomes arrive at the poles of the spindle, the nuclear membrane reforms, the chromatin expands, and the cytoplasm

divides. It is this stage in the process, when the cytoplasm divides, that is the focus of my research. This step, called cytokinesis, includes the furrowing of the cell, in which the contractile ring pinches off to place one nucleus in each cell. With the accomplishment of this step, two new daughter cells identical to the parent cell have been formed.

Progress through the cell cycle is achieved by two different cell cycle control mechanisms. These two mechanisms ensure correct advancement through the cell cycle by regulating the cell cycle machinery. The first type of control involves a series of phosphorylations by kinase enzymes and dephosphorylations by phosphatases that activate or inactivate proteins and complexes that initiate and regulate phases of the cell cycle. These kinases that participate in phosphorylation combine with cyclins to become enzymatically active. The activation/de-activation of these cyclin-kinase complexes trigger and help time various cell cycle events (Alberts et al., 2004).

A second type of cell cycle regulation is checkpoint control. It is not an essential part of the cell cycle, but is more supervisory. Specific checkpoints throughout the cycle sense flaws in critical events of the cycle. If one of the steps is delayed, or a flaw is detected, such as abnormal size, the control system will delay the activation of the next steps until the intracellular and extracellular conditions are favorable (Collins et al., 1997). There are two such checkpoints in the cell cycle that serve as molecular brakes. The first checkpoint lies in the G<sub>1</sub> phase and detects damage of the DNA. If the cell arrests in this phase, the cell has time to repair the damaged DNA before replicating it in the S phase. Another important cell-cycle checkpoint occurs in mitosis to ensure that all of the chromosomes are appropriately attached to the mitotic spindle. If not all of the

chromosomes are attached to the spindle, the cell could proceed through mitosis with the chromosomes unevenly segregating to the poles of the cell. With both of these checkpoints in the cell cycle, mutations and potential damage can be averted. Thus, the cell cycle's control system regulates and monitors the completion of critical events and can delay the progression, if necessary.

There are also additional checkpoints within the cell cycle, independent of the regulation of cell cycle machinery, which control such things as the actin cytoskeleton. According to Nakaseko and Yanagida (2001), cells have the ability to keep track of their actin cytoskeleton; if it is defective, the mitotic spindle during mitosis will become incorrectly oriented and the cell will suppress subsequent phases of cell division. The mitotic spindle, which serves to move the duplicated chromosomes apart during mitosis (Alberts et al., 2004), has its own separate checkpoint, which has been previously mentioned. Though defects in the mitotic spindle are associated with a checkpoint of the actin cytoskeleton, the two checkpoints are independent. What and how the actin cytoskeleton checkpoint monitors has not been completely determined. It is known that this checkpoint has the ability to block normal separation of sister chromatids, which can halt progression in the cell cycle, until the organization is correct. However, not much is known about the exact mechanism by which actin affects the spindle orientation. It has been proposed that when the actin-based cytoskeleton becomes damaged or disorganized, this somehow results in the spindle becoming misoriented, which in turn activates the Sty1/Spc1 protein (Nakaseko and Yanagida, 2001). The Sty1/Spc1 protein is a mitogen-activated protein kinase that phosphorylates another protein called Atf1, which is involved in a stress-activated protein kinase pathway. While the exact mechanism for this is not

known, it is clear that this stress-activated pathway is a key component of the actin-dependent mitotic checkpoint. The ultimate result of this pathway is a failure to segregate the duplicate chromosomes, which like any other checkpoint, delays cell division until the organization becomes corrected.

Cell volume is additionally regulated and controlled by specific pathways and points in the cell cycle. In eukaryotic cells, growth is regulated by extracellular growth factors in both gap phases,  $G_1$  and  $G_2$ , of the cell cycle. While there is no definite cell-size checkpoint, there is a system that regulates and maintains cell size that is related to the process of S phase initiation (Cooper, 2004). It has been proposed that mammalian cells initiate S phase and DNA replication at some relatively constant cell size (initiation mass), coupled with relatively invariant S and  $G_2$  phase times and variant interdivision times. Thus, the cell cycle age at initiation of S phase will occur earlier and earlier within the cell cycle as the growth rate of a cell increases (or as the interdivision time decreases), because the cell has quickly reached the proposed initiation mass. Because of this, faster growing cells will have a relatively short  $G_1$  phase and become larger than average cells, making the faster growing cells divide sooner because they reach the initiation mass earlier. In addition, smaller than average cells will delay initiation until the initiation mass is achieved. A cell that initiates S phase earlier in the cell cycle will have more time to increase its total mass prior to division, and conversely, smaller cells will delay initiation of S phase to allow for mass increase before the actual cell division. According to Cooper, this finding suggests that normal cells must operate some sort of checkpoint in order to maintain a constant average cell size; the checkpoint ensures that a cell does not continue to grow after a certain size, until after division. While this cell-size

checkpoint operates to prevent cells from getting progressively bigger and bigger, there is presumably another checkpoint that prevents division from occurring before the cells have reached an adequate size, in order to prevent them getting progressively smaller.

### *Cytochalasin B*

Cytochalasin B is an alkaloid metabolite of the mold *Helminthosporium dematiodeum* produced by mold to kill off bacteria. It is known to inhibit a wide variety of cellular movements including cytokinesis, cell locomotion, cytoplasmic streaming, blood clot retraction, and movements associated with developmental processes (Lin et al., 1973). Brown and Spudich (1981) reported that cytochalasins inhibit the rate of actin assembly. Lin, Santi, and Spudich showed earlier that cytochalasin B inhibits actin assembly by causing a decrease in the intrinsic viscosity of actin, and an altering in the morphology of the actin filaments, as shown in muscle and blood platelets (Lin et al., 1973). They also suggested that there could be a possible cytochalasin B receptor on actin microfilaments. Because they were able to show that there is a concentration dependence on binding of cytochalasin B to different types of cells, they concluded that there are at least two types of binding site for cytochalasin B, as shown by their results using bovine platelets, HeLa cells, bovine red blood cells, *D. discoideum* amoebae, and *A. aereogenes* cells (Lin et al., 1973). Lin, Santi, and Spudich (1973) named these sites high and low affinity-binding sites. Flanagan and Lin next observed that in fact, filamentous actin (F-actin), and not globular actin, contained such high affinity cytochalasin B binding sites (Flanagan

and Lin, 1980). This F-actin lies at the end of the filament where assembly takes place, blocking the assembly end (Brown and Spudich, 1981). In our lab, we are making use of these observations and the previous research done on cytochalasin B to induce U937 leukemia cells into multinucleation. Multinucleation is the process by which the actin microfilaments in cytokinesis are disrupted, resulting in a cell accumulating more than one nucleus.

*Manipulation of the cell cycle's regulation: induction into multinucleation*

Normal cells have key checkpoints in the cell cycle that signal the cell to either delay progression until any abnormalities are corrected, or to continue through the cycle with no interruption. If cytochalasin B was used on a population of normal, non-neoplastic cells, the cells would halt at the second checkpoint and direct the cell to stop dividing. This is due to the fact that cytochalasin B prevents normal cells from entering the cell cycle because it disrupts the actin microfilament cytoskeleton. The control system of the cell cycle will delay the activation of the next steps, and the cell will stop dividing mitotically in order to correct the shape and integrity of the actin cytoskeleton before allowing entry back into the cell cycle (Law and Reed, 1995). In some neoplastic cells, on the other hand, actin microfilament disruption induced by cytochalasin B does not prevent cell cycle entry, but after completion of the cell cycle and nuclear replication, the absence of a functional actin cytoskeleton does prevent cytokinesis. The neoplastic cells have lost the key mechanism for controlling entry into the cell cycle, and multinucleation will result. The neoplastic cell will go into the cell cycle and make DNA, but will not be able to

split into separate cells, thus creating multinucleation and enlargement of the cells. Thus while normal cells exit the cell cycle and enter a G<sub>0</sub> (resting) state, neoplastic cells continue nuclear division, become extremely enlarged and heavily multinucleated, and are also likely to contain elevated numbers of mitochondria per enlarged cell.

We hypothesize that enlarged cells containing high levels of DNA and high mitochondrial contents may enter apoptosis more readily when they experience DNA or mitochondrial damage than will cells with normal amounts of DNA and mitochondria. This could occur because the enlarged cells have more targets per cell for damage by DNA-directed agents or by agents damaging mitochondria. We further hypothesize that enlarged leukemia cells may be more susceptible to physical damage than are normal-sized leukemia cells because of the increased cytoplasmic volume retained by a plasma membrane with weakened internal cytoskeletal support. In our research, we have found that U937 human promyleocytic leukemia cells that have been treated with cytochalasin B become heavily multinucleated, containing as many as eight or more nuclei depending on the length of treatment time. U937 leukemia cells were chosen for this study for two main reasons. The first characteristic of these cells that makes them ideal for our experiments is the fact that they do not adhere to one another, making them easy to count and individually to size. Also, the U937 leukemia cells have the ability to grow in suspension, rather than attached to the plastic culture flask, again making them easier to count and size reliably. With a high number of nuclei in one single cell, we think that the internal cytoskeletal support might weaken, and propose that sonication of the multinucleated cells may make them more susceptible to apoptosis-induction.

### *Ultrasound-induced cavitation*

In medicine, ultrasound has been a widely used and well-established diagnostic and therapeutic technique for many years (Liu et al., 1998).

Ultrasound is commonly used for soft tissue imaging because of its perceived safety, noninvasiveness, and low cost (Feril Jr. and Kondo, 2004). Ultrasonic-imaging, which uses high-frequency low-intensity ultrasound, is used to scan organs and visualize their size and structure. This type of ultrasound does not damage the skin or sonicated organs. At somewhat greater intensities, ultrasound can be used therapeutically to heat tissues deep within the body. On the opposite end of the frequency spectrum, low frequency and high intensity focused ultrasound is often used in lithotripsy, a procedure used to break up kidney stones within the body so that they can pass without the need for surgery (Liu et al., 1998).

Medical ultrasound has many other applications, including cancer therapy, which involves the process of acoustic cavitation (Feril Jr. and Kondo, 2004).

Acoustic cavitation is the process by which high intensity acoustic fields in liquids lead to the creation and oscillation of cavities or gas bubbles (Liu et al., 1998). Acoustic cavitation has been shown to increase the permeability of cell membranes. This form of cavitation has been used to permeabilize cell membranes, making it easier for materials to enter the cells without damaging them (Lee et al., 2004). Others have shown that ultrasound transiently disrupts cell membranes facilitating the loading of drugs and genes into viable cells (Cochran and Prausnitz, 2001).

The goal of my laboratory use of ultrasound is not for drug delivery. Rather, it is to determine whether there is a sonic sensitivity of cells enlarged by treatment with cytochalasin B that might be exploitable as a potential modality in leukemia therapy. Using acoustic cavitation, we have developed procedures with the potential to differentially target the enlarged U937 leukemia cells created by treatment with cytochalasin B possibly increasing their sonic sensitivity in comparison with untreated control cells. This physical treatment may be applicable to enhancing the cytotoxic effects of microfilament agents in treatment of leukemia in pre-clinical animal models.

## METHODS

### *Cytochalasin B enlargement of U937 leukemia cells*

U937 leukemia, a human promyleocytic cell line, was used in this work. Cells were seeded at  $5.0 \times 10^4$  cells/ml in 20% fetal bovine serum in Iscove's medium supplemented with 2% of 10,000 units penicillin and 10 mg streptomycin, 0.5% gentamicin sulfate, and 2 mM glutamine. The cells were treated with cytochalasin B at concentrations ranging from 1.25  $\mu\text{M}$  to 2.1  $\mu\text{M}$  and were allowed to proliferate and enlarge for thirty-six hours. After thirty-six hours, the cytochalasin B-treated cells were spun down in a 50 ml centrifuge tube. The tube consisted of 30 ml of cells placed carefully on top of 20 ml of phosphate buffered saline medium (PBS) at 37°C. The tube was spun for two and a half minutes at 20 G. The size distribution and cell number of the enlarged, multinucleated cells were determined with a hemocytometer using the trypan blue dye exclusion test procedure and with a Model Z1 Beckman-Coulter Particle Counter for both the supernatant and precipitate. This procedure is outlined below. Figures 1 and 2 below show (without trypan blue) a population of control U937 leukemia cells in a hemocytometer at 100X as well as after treatment with cytochalasin B.

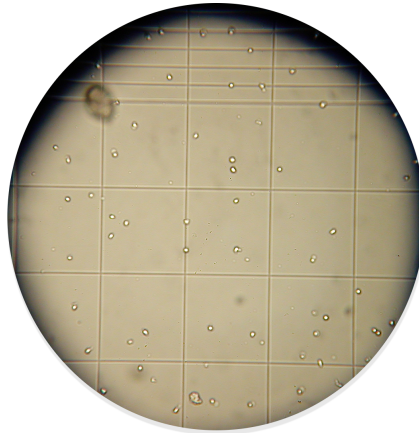


**Figure 1:** A population of un-treated control U937 leukemia cells.

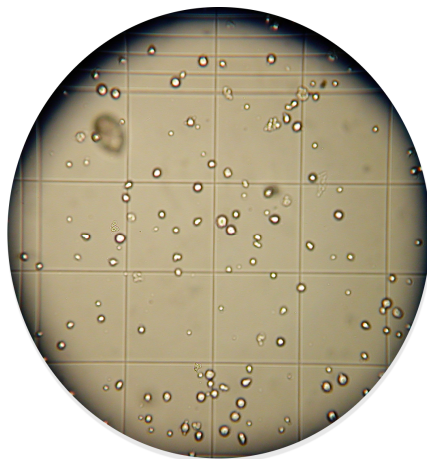


**Figure 2:** A population of cytochalasin B treated U937 leukemia cells.

#### *Filtration and separation of cells*

The precipitated enlarged CB-treated cells were then filtered through nylon mesh sieve to separate the enlarged, multinucleated cells from the unenlarged, mononuclear cells. A 4.5 cm filter was used fitted with 20  $\mu$  nylon mesh for the sieve. A 12.5 ml aliquot of cell suspension was added to the sieve and was then allowed to filter until the flow of the cell suspension through the filter slowed to one drop a minute. The filtrate was then removed and saved in a

25 ml tube to later determine its size distribution. The trapped cells on the sieve were re-suspended and washed in 5 ml of warm equilibrated medium. Ten ml of additional cell suspension was added to the sieve and was filtered as above. The trapped washed cells were re-suspended once again after the second 10 ml was filtered. The filtrate and trapped cells were counted and sized using the hemocytometer and Coulter Counter. Both of these procedures are outlined below.

Results from this separation procedure (see Results) provided experience with ways to improve the separation of the enlarged cells from normal sized cells. The filtration procedure was improved based on my results with the 20  $\mu$  nylon mesh separation. Dr. Thomas Fondy designed a cell separation procedure to better separate the enlarged, multinucleated cells from the mononucleated cells for use in the sonication experiment below. For this separation procedure, U937 leukemia cells were seeded at  $3.4 \times 10^4$  cells/ml in 20% fetal bovine serum in Iscove's medium and were treated with cytochalasin B at a concentration of 1.25  $\mu$ M and allowed to proliferate and enlarge for thirty-six hours. Twenty-four ml of the cells were centrifuged on top of 30 ml of warm PBS in a 50 ml centrifuge tube at 20 G for 3 minutes. The upper 40 ml were removed and saved and the bottom 10 ml fraction was saved as the 20G precipitate.

A 19  $\mu$  nickel porated sieve was placed inside a crystallizing dish and cold sterile PBS was added to 0.5 cm above the top of the sieve. The 10 ml fraction from the 20G precipitate was added to the sieve and was allowed to settle in a refrigerator for 30 minutes. The upper fraction from the sieve (46 ml of cells in PBS suspension) was recovered. Ten additional ml of PBS was added to the sieve

and the 46 ml recovered was re-sieved and allowed to settle in a refrigerator for 30 minutes. From atop the sieve, 60 ml was recovered and saved as the trapped fraction and 42 ml was recovered from the bottom of the sieve and saved as the filtrate. The trapped fraction was centrifuged in two 50 ml centrifuge tubes at 20 G for 3 minutes. The upper 30 ml from each tube was removed, which left 500 µl in the bottom of the two tubes. To the 500 µl, 5 ml of 20% FBS in Iscove's medium was added to both tubes and they were combined to give a total of 11 ml. Ten ml was taken to form the final trapped fraction, which was diluted with 11 ml of 20% FBS in Iscove's medium to give 21 ml of  $1.95 \times 10^4$  viable cells/ml for use in the sonication experiment.

#### *Ultrasonic disruption*

Once the cells had been separated through use of the sieve, the cells were then subjected to ultrasound. To create the ultrasound delivering apparatus, an Omega pro lab timer was connected to an E/MC model 250 ultrasonic bath cleaner with a measured mean output of 0.77 watts (see Appendix E). The ultrasound bath was filled with 250 ml of distilled water at 37°C. A ring stand was also used to hold the tubes exactly at the focus point of the sonicator. Trapped cells were suspended at  $2.0 \times 10^9$  viable cells/ml in 20% FBS with Iscove's medium. Two ml aliquots were placed in 8 ml sterile tubes (100 mm x 12 mm). The tubes were then sonicated at 0, 2, 4, 6, 8, and 10 seconds and were done in duplicate. Un-enlarged and untreated leukemia cells at  $2.0 \times 10^4$  viable cells/ml were used as the control and were sonicated at the same lengths of time as the CB-treated trapped fraction, as well as being done in duplicate. Each tube's

sample was gently re-suspended and was placed in the water so the 2 ml sample was completely submerged. After all of the tubes had been sonicated, samples were taken from each tube for hemocytometer counts to determine cell viability and re-growth (see procedure below).

### *Determining cell viability*

Determining cell viability of the U937 population was done using a trypan blue dye exclusion test coupled with a hemocytometer. Trypan blue is one of several stains used in this method, which is based upon the principle that viable cells do not take up the dye whereas non-viable cells do. This occurs because cells with an intact membrane are able to exclude the dye while cells without an intact membrane take up the trypan blue. Therefore, all cells that exclude the dye are scored as viable. The test was performed by mixing 50 µl of cell suspension with an equal amount of 0.4% trypan blue stain in isotonic saline. After the stain was added, the solution was mixed thoroughly and 12 µl of the mixture was transferred to each of the two counting chambers of a hemocytometer. By means of a light microscope, the cells were recorded as either small (<20 µ) or big (>20 µ) in size using the eyepiece reticle, and whether they were viable or not. Using a trypan blue viability form created in Microsoft Excel and developed by Dr. Thomas Fondy (see Appendix A), the total percent viability and cell size were calculated for the population. Figure 3 below shows an example of a slide that contains both enlarged, multinucleated cells and un-enlarged cells, and that have either taken up or excluded the dye.

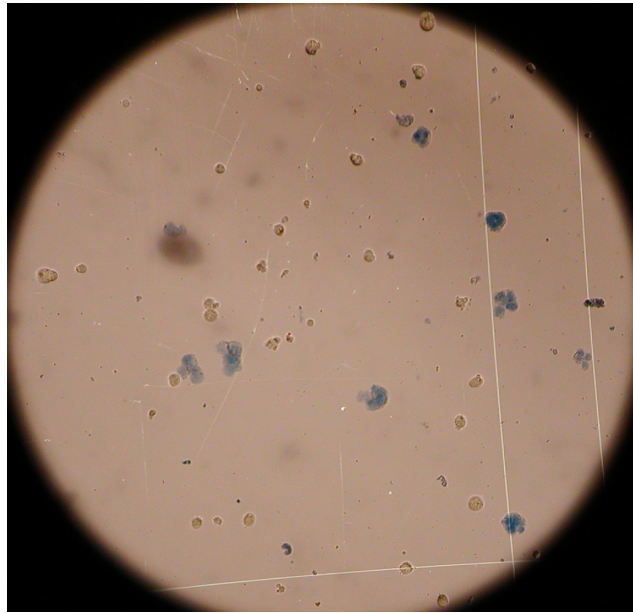


**Figure 3: A population of viable and non-viable cytochalasin B treated U937 leukemia cells.**

*Measuring cell size*

The size distribution of the cell suspension was determined using the Coulter Counter. The Coulter Counter is an instrument designed to analyze particle size by calculating the measurable changes in electrical resistance produced by nonconductive particles suspended in an electrolyte. Using a small round-bottomed cuvette, 1 ml of cell suspension was added to 14 ml of isotone for a dilution factor of 15. A blank was also prepared with 15 ml of isotone and was run first before the samples to ensure that the background particle count was low. The instrument was set at a desired particle threshold to obtain the number of cells that are equal to or bigger than the setting (for example,  $\geq 19 \mu$  finds the total number of cells that are at least  $19 \mu$ .) The aperture tube was flushed between each analysis and the sample was gently stirred with a glass rod to evenly re-

suspend the cells, but to avoid damaging the cells or getting air bubbles. A 0.5 ml sample was counted. The cell number per ml was determined by multiplying the particle count by 2 and by the dilution factor. Dr. Thomas Fondy developed Coulter Count forms using Microsoft Excel (see Appendix B), which allowed us to determine the number of cells at each increasing micron from 10  $\mu$  to 30  $\mu$  and also calculate the percentages of cells of various diameters.

#### *Determining nuclear content*

The number of nuclei in a cell was determined by DAPI (4', 6-Diamidino-2-phenylindole) staining techniques. The DAPI stain was used because it could form fluorescent complexes with natural double-stranded DNA. The procedure involved mixing 1 ml of cells at a density of  $1 \times 10^5$  cells/ml with 0.5 ml of 10% formalin solution. Formalin was used because it has the ability to kill and fix the cells so that they would maintain their shape and structure without loss of nuclear content. The cells were left in the formalin overnight, and the next day the suspension was centrifuged for 90 seconds at 1,500 RPMs, or 500 G. Care was taken not to exceed 2,100 RPM because this may damage the cellular integrity. The cells appeared as a small pellet on the bottom of the microfuge tube. The supernatant was removed and 5  $\mu$ l of DAPI (concentration 1  $\mu$ g / $\mu$ l) was added to the pellet. After being carefully mixed, 5  $\mu$ l of the cells in the DAPI suspension were added to a slide and the slide was sealed with a cover slip. Under a fluorescent microscope, the number of nuclei in each cell was recorded. Figures 4

and 5 show visual differences in the number of nuclei seen in both small, mononuclear U937 cells and enlarged, multinucleated U937 cells.



**Figure 4: U937 leukemia cells that have been enlarged and multinucleated by treatment with cytochalasin B.**

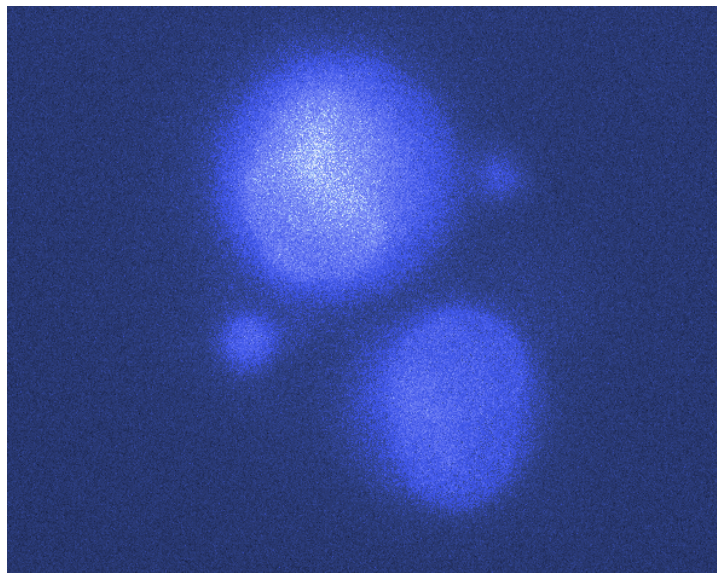


**Figure 5: Control mononucleated U937 leukemia cells.**

## RESULTS

### *Separation of the enlarged, multinucleated cells*

The effectiveness of the separation technique using the 20  $\mu$  nylon mesh sieve was determined by measuring the percentage of all trapped •19  $\mu$  cells in comparison with the percentage of all •19  $\mu$  cells in the unseparated population and in the nylon mesh filtrate. The percentages of total cells sieved that were recovered in the trapped and filtrate fractions were determined in a recovery analysis. The dye exclusion viability and extent of multinucleation were determined for the trapped fraction. The cell sizing and counting were done using a Coulter Counter and hemocytometer (see Methods). Before the cell suspension was sieved, the proportion of cells that were •19  $\mu$  was 67%, as seen in Table 1 and Figure 6, and the trypan blue viability was 77%. After the filtration, the proportion of cells •19  $\mu$  in the filtrate was reduced to 52%. This population was 74% of the total sieved. The trapped cells showed 44% of the cells were •20  $\mu$ . A Coulter count at 19  $\mu$  was not done for the trapped cells. The trapped portion showed 82% trypan blue viability. Of the viable cells, 93% were enlarged (•20  $\mu$ ). Thirteen percent of the total cells sieved were recovered in the trapped fraction. The total recovery in the filtrate and trapped fractions was 87%. This data can be seen in Table 1 below.

**Table 1: 20  $\mu$  Nylon Mesh Separation of CB-Treated U937 Leukemia Cells**  
(1.0  $\mu$ M CB, 3 days, 10% FBS Medium)

Fraction	Volume (ml)	Total Cells/ml (in $10^4$ units)	Total Cells (in $10^4$ units)	Recovery (%)	Trypan Blue Viability	Cells 15 $\mu$ to 19 $\mu$ (% of Total)	Cells >19 $\mu$ (% of Total)	Cells >25 $\mu$ (% of Total)
Unseparated	22.5	1.8	40.5	100	77%	33	67	26
Filtrate	~30	1.0	30	74.1	-----	48	52	19
Sieve Trapped	~13	0.4	5.2	12.8	82%	56	44	37

The trapped fraction from the sieve contained a higher percentage of the biggest cells ( $>25 \mu$ ) than the filtered fraction, as seen in Table 1 and Figure 6. Thus, the nylon mesh sieve did preferentially trap the bigger enlarged cells.

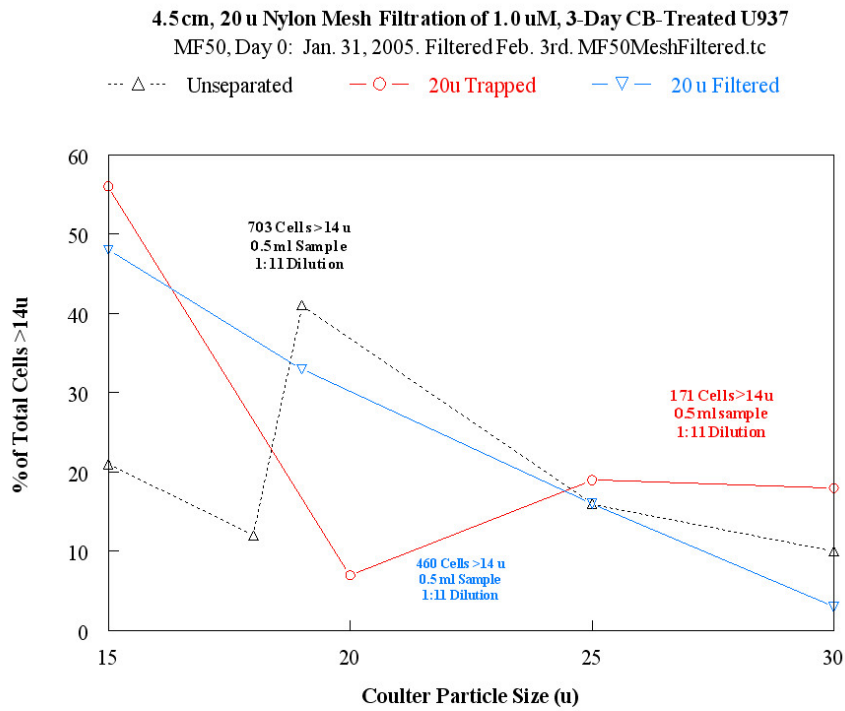


**Figure 6: Percent of total cells  $>14 \mu$  of the unseparated CB-treated U937 leukemia cells and the trapped and filtered fractions after sieve separation.**

*Ultrasonic disruption of the U937 leukemia cells*

To determine whether there was a sonic sensitivity in cells treated with cytochalasin B, control U937 cells and CB-treated U937 cells, taken from the  $>19 \mu$  trapped fraction after separation, were exposed in duplicate to ultrasound at a power of 0.77 watts for varying lengths of time, specifically, 0, 2, 4, 6, 8, and 10 seconds (only one tube was exposed to 10 seconds). The data for the CB-treated cells can be seen in Appendix C. (The controls are not listed.) Data are shown for 0, 2, 4, 6, 9, and 11 days post-sonication; however, both CB-treated tubes sonicated at four seconds and the single CB-treated tube sonicated for ten seconds could not be counted at 11 days due to mold growth. In addition, one tube at four seconds and one tube at ten seconds for the controls had mold growth by day 9, so the data used is only for one tube at day 9. The controls reached confluence by day 6 and the CB-treated cells reached confluence by day 11, so the effect of late-stage mold growth in these tubes is of minor importance.

In the regrowth counts for the CB-treated enlarged cells, by day 9, the proportion of cells that were  $>19 \mu$  were between 2% and 14%. By day 11, no viable big cells were seen in the 0, 2, 6, and 8 second tubes, the tubes that had no mold growth. This can be seen in Figure 7.

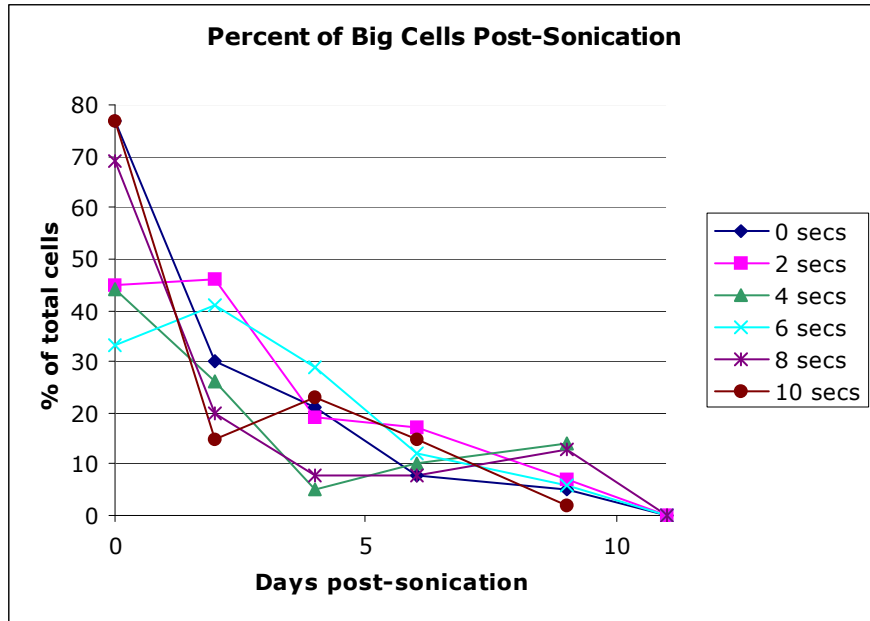


**Figure 7: Percent of Big Cells Post Sonication.**

As seen in Figure 7 and Appendix C, the percent of the total enlarged, big cells for the CB-treated tubes decreased overall as a function of the length of time (in days) post-sonication. As the number of elapsed days after sonication increased, the initial viable big cells either died or may have turned into small cells due to cell division. By day 9, the average percent of trypan blue positive (dead) enlarged cells was 58%, compared with 11% for day 2. The few viable big cells seen on day 9 could have been mitotic cells that were dinucleated and enlarged; normal U937 leukemia cells typically have around 3% of their cells enlarged due to mitosis.

After the tubes were sonicated at their respective time intervals on day 0, the initial day 0 counts were determined as the initial reference point for later regrowth counts, and also to determine whether sonication affected cell size distribution, especially in the enlarged CB-treated tubes. As seen in Figure 8, there was a fairly consistent effect on the number of big viable cells per milliliter

immediately after sonication. While the number of big cells per milliliter did decrease from 0 seconds of sonication (i.e. no sonication) to 6 seconds and they increased again from 6 to 10 seconds of sonication, showing no clear trend. However, combining all nine sonicated tubes versus the non-sonicated, 0 second tubes shows an average of a 71% decrease of big viable cells per milliliter as a result of sonication, suggesting that there was an effect.

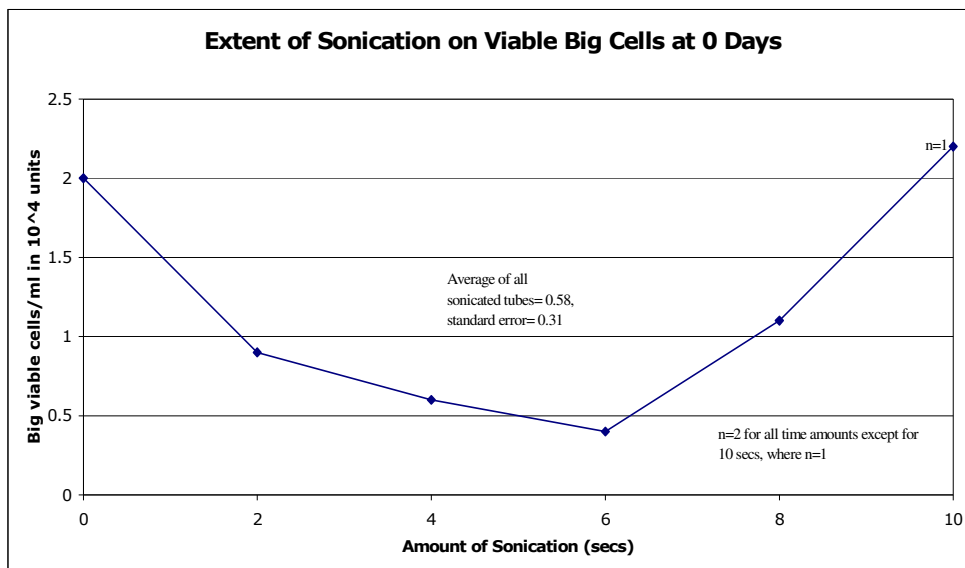


**Figure 8: Viable Big Cells Immediately After Bath Sonication.**

In addition to decreasing the proportion of big viable cells, sonication also affected the subsequent growth rate of the CB-treated cells. The cell counts at day 2, most notably, seem to show that the growth of the viable cells was progressively inhibited by increasing the time of sonication. This can be seen more clearly in Table 2, which tabulates the number of cells per milliliter on day two as a function of the amount of sonication. The growth rate of the cells does decrease as the amount of sonication is progressively increased, reaching a maximum 76% retardation of growth at six seconds.

**Table 2: Day 2 Regrowth Counts showing the retardation in the growth rate**

Amount of Sonication (secs)	Viable cells/ml in $10^4$ units	% of 0 secs growth rate	Amount of growth rate retardation (%)
0	6.56	-----	-----
2	6	91	9
4	4.78	73	27
6	1.56	24	76
8	2	30	70
10	3.56	54	46

Figures 9 and 10 show logarithmic plots of the concentration of viable cells from the CB-treated tubes and for the control cells for different amounts of sonication. Comparing the two figures, there seems to be a retardation in growth rate for the CB-treated tubes that persisted throughout the period of observation. Both the non-sonicated CB-treated cells and the non-sonicated control cells grew to confluence, but the control cells reached this point roughly four days earlier (day 6) than the CB-treated cells (~day 11). This delay in reaching confluence shows that enlarged purified CB-treated cells retain viability, but have a lower growth fraction and/or a longer cycling time than control U937 cells exhibit. This is consistent with cloning efficiency determinations by Dr. Thomas Fondy where the control U937 cells show 50% cloning efficiency, while the trapped cells show a cloning efficiency of 5% to 8%.

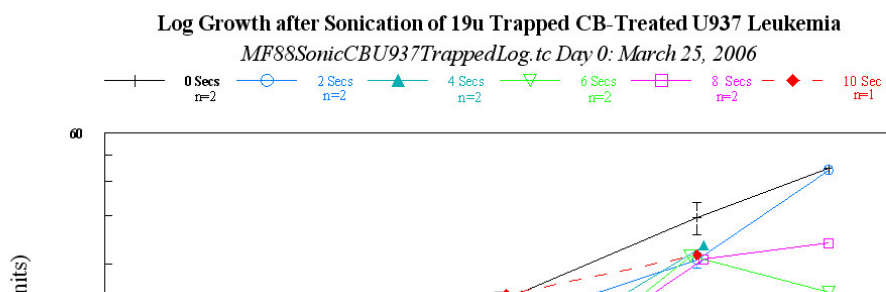


**Figure 9: Regrowth of the U937 CB-Treated Small Cells after Bath Sonication.**

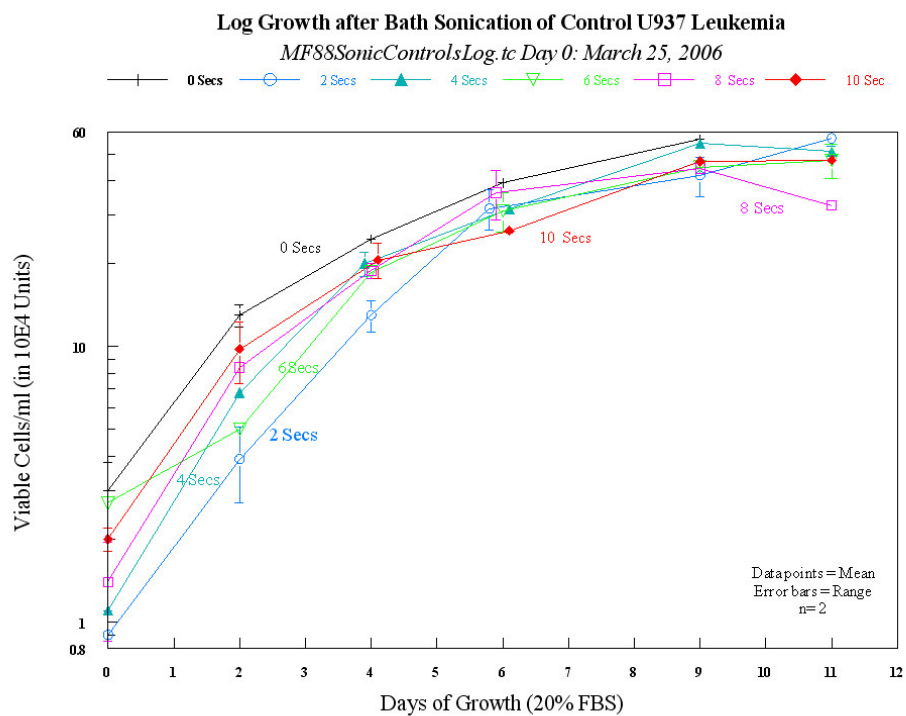


**Figure 10: Regrowth of the U937 Leukemia Control Cells after Bath Sonication.**

The most clear cut evidence of a retardation in growth rate related to the amount of sonication can be seen by averaging together the means for 0 and 2

seconds and comparing these results to the comparable average means for 6 and 8 seconds. (Performing these averages improves the statistical significance of the result.) In Figure 11 which plots the growth after sonication of the control leukemia cells, there is no statistically significant difference between the average of the means of the number of viable cells per milliliter of the 0 and 2 second tubes versus the average of the means of the 6 and 8 second tubes.

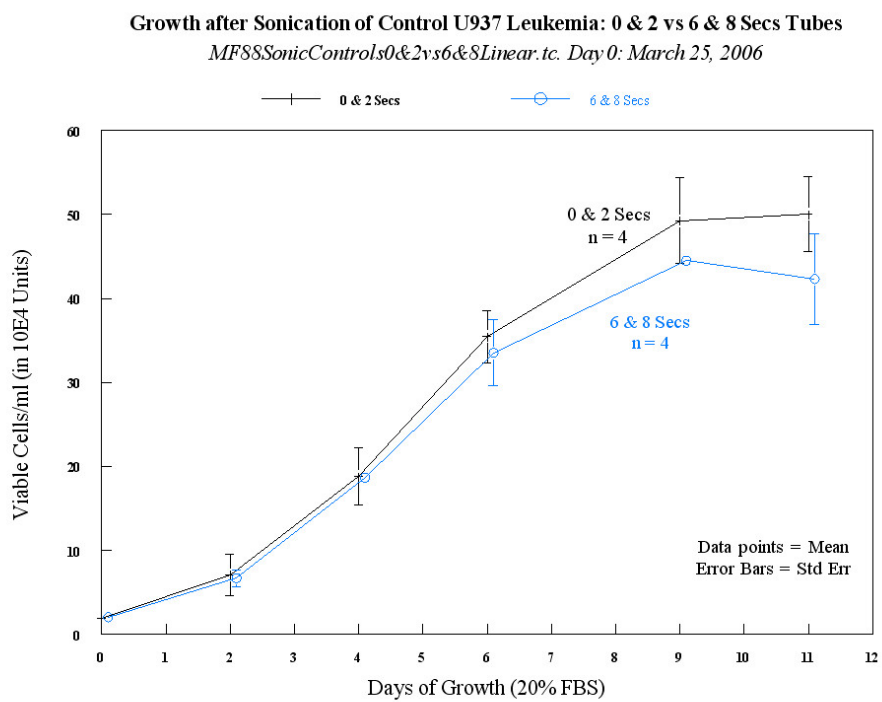


**Figure 11: Regrowth after Sonication of Control U937 Leukemia Cells, 0 & 2 secs vs 6 & 8 secs Tubes.**

However, when the same comparison is made with the CB-treated leukemia cells in Figure 12, a statistically significant difference can be seen between the means of the 0 and 2 second data versus the means of the 6 and 8 second data, based on t-tests that were performed on the data for each observation time. The differences on days 2 and 6 are statistically significant at p-value=

0.005 and p-value= 0.02, respectively (Day 2 t-statistic=4.09, Day 6 t-statistic=3.04, df= 6). Days 4 and 9 are not statistically significant. Data at day 11 was not included due to mold growth, which lessened the sample size.

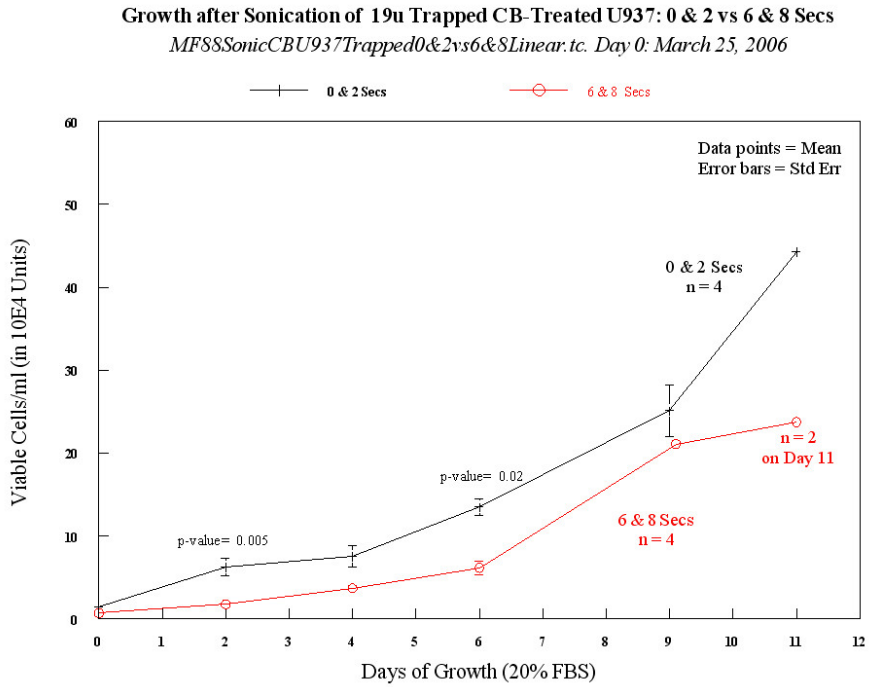


**Figure 12: Regrowth after Sonication of CB-Treated U937 Leukemia Cells, 0 & 2 secs vs 6 & 8 secs Tubes.**

Figure 13 plots the total number of dead control U937 leukemia cells as a function of days post-sonication. Examining this figure, and excluding day 11, there seems to be no effect of sonication on the control cells after day 0 since the percent of dead cells remains approximately constant as a function of time at all levels of sonication. (On day eleven, all the samples show an elevated count of dead cells, perhaps because the cells had been at or near confluence for five days.) There does, however, seem to be initial damage on the controls, evident by the high percentages of trypan blue positive cells on day 0. Nevertheless, the highest percentages of dead cells are in the 2, 8, and 10 second tubes, which only had 11,

20, and 24 cells counted in the hemocytometer for 18 fields each, respectively. (On later days, there was not a problem of a small sample size because the counts were much larger.) Thus, sonication might have had an initial effect on the control cells, but since the samples are so small, it is hard to tell if the effect is real. If it is, it disappeared by day 2 once the cells began growing toward confluence.

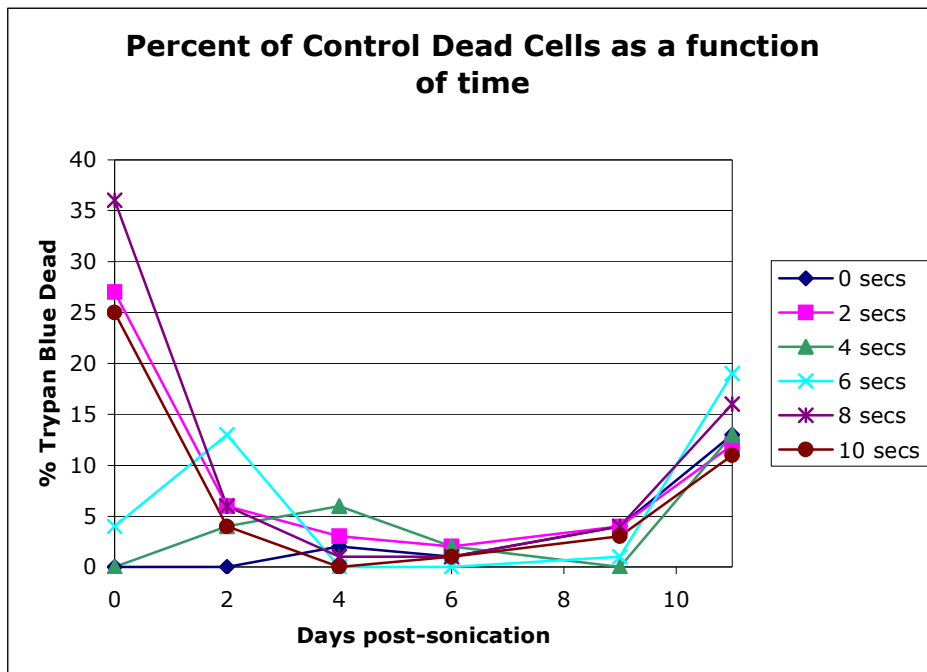


**Figure 13: Percent of Total Dead Control U937 Leukemia Cells as a Function of Days Post-Sonication.**

The percent of CB-treated dead cells seen in Figure 14 shows a distinct difference in the pattern of dead cells compared to the viability of sonicated control cells. Although the CB-treated cells were initially damaged immediately after sonication, just as the controls were, beginning at day four, the percent of dead CB-treated cells for 8 and 10 seconds of sonication does seem to increase and stay relatively higher than the non-sonicated CB-treated cells. Thus, there

does seem to be a slight dose-dependent effect for the sonicated CB-treated cells that was not seen in the sonicated control cells. This higher death rate is also consistent with the lower growth rate of the CB-treated cells seen previously in Figure 9.

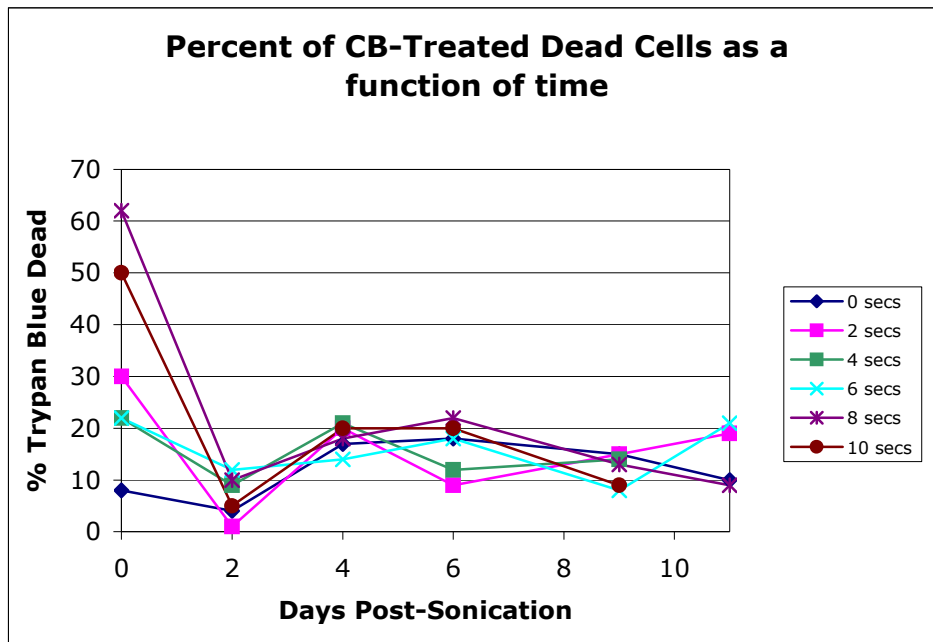


**Figure 14: Percent of Total Dead CB-Treated U937 Leukemia Cells as a Function of Days Post-Sonication.**

## DISCUSSION AND CONCLUSION

### *Separation of the enlarged, multinucleated cells*

A great deal has been learned from our separation experiments and we have utilized some new ideas to enhance our methods of filtration and purification of enlarged multinucleated cells. In the separation experiment we performed using the 20  $\mu$  nylon mesh sieve, the trapped fraction contained approximately a 52:44 ratio of small and big cells, respectively. Since >50% of the trapped fraction was still composed of cells <19  $\mu$ , the 20  $\mu$  sieve trapped a substantial proportion of cells smaller than 20  $\mu$ . This large percentage of small cells trapped by the filter may have resulted because big cells blocked the filter holes so the small cells could not flow through. We observed that the cells collected around the edges of the mesh filter and were able to obstruct passage. Some cells larger than 20  $\mu$  passed through the nylon mesh. Big cells that were not trapped by the filter may have gone through the filter because of its range of hole sizes ( $20 \pm 7 \mu$ ) or because they were physically forced through it by net hydrodynamic flow. Since the big cells have disrupted actin microfilaments, they are likely to be deformable.

The separation technique was a bit more effective for cells that were roughly • 25  $\mu$  since the trapped fraction contained a larger percentage of 25  $\mu$  cells than the filtrate did, as seen in Figure 6. The filtration method was most effective for the largest of the big cells (30  $\mu$ ). Although the trapped fraction only contained 44% enlarged and multinucleated cells, the experiment suggested modifications to our sieving procedures that were in fact highly effective. We

have modified many different aspects of the method in developing our improved procedure (see Methods) to enhance and maximize the purification.

The first modification we made is probably the most important change in regards to how the cells behave during filtration. We had previously noticed that when the cells were added to the filter, the big cells were forced through the filter by hydrodynamic flow. There also seemed to be many holes in the filter that were blocked, suggesting occlusion and termination of flow. We now allow the cells to settle through a continuous volume of phosphate buffered saline while filtrating with no net hydrodynamic flow, rather than letting them simply drip through the filter in a flowing medium. To do this, we use a crystallizing dish as a holder and place the sieve within it. With a continuous liquid volume around the sieve, no cells are forced through and have the chance to settle through the filter on their own with no pressure involved. Before adding the cells, the sieve is submerged in PBS until the liquid level is roughly 1 cm above the top of the sieve. Once the cells are added and begin to settle through the medium, there is no net flow through the filter and there is less of a chance for the big cells to be pushed through by heavier cells above them. We did observe in the microscope that the trapped cells bounced up and down above the sieve perforations and did not occlude them.

Following the adaptation to the sieve apparatus, it occurred to us that the procedure could be further improved if it were possible to partially separate the cells before they were applied to the sieve. To do this, we began centrifuging the cell suspension at different forces and durations to see what combination gave the optimal separation of big and small cells in the precipitate and supernatant. After experimenting with centrifugation of the cells, it was determined that a speed of

200 RPM, or 20 G, was the ideal force for a period of 2 minutes. By centrifuging the cells before they are added to the filter, we can preferentially leave the small cells behind and concentrate the precipitate with big, multinucleated cells. Once the concentrated cell suspension is added to the filter, it would also be easier to see the direct effect of the sieve on the multinucleated cells if there were fewer small cells present in the initial cell population added to the sieve.

Another modification to the filtration method we made was unit gravity sedimentation of the cells before they are applied to the filter. The cell suspension is first added to a syringe attached with a leur lock valve and then room temperature PBS is added on top of the suspension to give the cells a medium to settle in. The syringe is then inverted to allow the big cells to settle near the plunger, and then the syringe is re-inverted so that the small cells are closest to the leur lock valve. By doing this we can initially separate the cells inside the syringe, thus allowing the small cells to come out first after the syringe is re-inverted and followed by the bigger cells. We believe that this could help improve the efficacy of the separation by allowing the small cells to pass through the sieve without being occluded by big cells. This unit gravity separation using a syringe can be used in conjunction with the centrifugation, or by itself, to preferentially separate the cells before filtration.

Another adjustment we made to our procedure was in the filter that was used to separate the cells. The filter originally used was a 20  $\mu$  nylon mesh sieve followed later with a 20  $\mu$  stainless steel mesh sieve. These filters had margins of error of about  $\pm 7 \mu$ . Thus, there was no guarantee that every perforated hole was exactly 20  $\mu$ . Since many of the holes may have been bigger than expected, this

could be the reason why some of the big cells were not trapped by the filter. After researching sieves and materials, we found a nickel electroporated sieve that promised to give better purification results. Because the sieve is made by an electroporating process that forms uniform holes in a nickel plate, rather than by weaving nylon or stainless steel mesh, it has a smaller margin of error ( $\pm 2 \mu$ ). The sieve also has round apertures (round holes) that are not possible with woven nylon threads or stainless steel wires. This provides uniform round perforations rather than rectangular openings to enhance purification.

In addition, we also think that the big cells might have been pushed through the filter because the room temperature PBS made the cells' cytoskeleton plastic and allowed the cells to deform without actually rupturing. To modify this and make the cells remain rigid, we now conduct the sieve purification at 4°C. Lastly, we have observed that when adding cold PBS to the sterile sieve, bubbles could collect underneath it. If this happened, many holes of the sieve were blocked and unable to let cells flow through them, as evidenced by microscopy. We now sterilize the sieve in distilled water to keep it wet. Before sieving the cells, we pour off the water and add cold PBS to the sieve in the crystallizing dish tipped to one side. This prevents any air bubbles from blocking the underside of the sieve. With all these modifications made, our procedure has allowed us to produce a population of CB-treated U937 leukemia cells that are 94%  $\bullet 19 \mu$  cells.

#### *Ultrasonic disruption of the U937 leukemia cells*

In our work, we attempted to exploit the enlarged size, weakened

cytoskeleton, and consequent increase in membrane fragility of CB-treated cells versus control cells in producing increased sonic damage to CB-treated leukemia cells. Previously, Dr. Thomas Fondy had found that Coulter counts showed a shift in size distribution of the CB-treated cells to smaller cells post-sonication (see Appendix D). In the present study, we have observed a similar effect of sonication on cell size (Figure 7). We also found that there was a statistically significant inhibition of growth in sonicated CB-treated cells at two and six days post-sonication in comparison with CB-treated cells not sonicated or given two seconds of sonication. However, further experiments would need to be completed to determine whether the growth inhibition and shift in size distribution found in the CB-treated cell population is reproducible and different from the effects of sonication on the control U937 leukemia cells.

Based on t-tests that were performed to assess whether the average means of the number of viable cells per milliliter for the combined 0 and 2 seconds data were statistically different from the combined 6 and 8 seconds data, we can say with 99.5% confidence that the average means of the 0 and 2 second data at day 2 for the sonicated CB-treated cells were statistically different from the average means of the 6 and 8 second data on the same day. In addition, the difference between the average means at day 6 was statistically significant at the 98% confidence level. Although the difference between the two data sets on day 4 was not statistically significant ( $p$ -value= 0.10), the data shows that there was a true retardation effect on the growth rate of the CB-treated cells by the sonication. Since there was no statistically significant difference seen on any day for the control data, we can be reasonably confident that there is a difference in sonic sensitivity of CB-treated enlarged cells in comparison with control U937

leukemia cells.

In addition, we observed that the percent of viable big cells was reduced as additional days passed following the sonication, compared to non-sonicated CB-treated tubes. Since the percentage of trypan blue positive big cells remained at around 10% or higher for up to six days, it is likely that sonication killed some of the enlarged CB-treated cells or split them into smaller cells. Viable enlarged cells would be expected to divide in the absence of CB. This is consistent with the reduction in cell size distribution as a function of sonication seen on day 0.

In our experiment we took data only every second day, and there was a three-day interval after day 6. It would improve the experiment if counts were taken at shorter intervals in order to determine when in fact, all the big viable cells disappear for each length of time that the tubes were sonicated. With more readings at shorter time intervals, an exact point of complete big cell disappearance could be determined, which could make it easier to see if there really is a clear effect that correlates with the amount of sonication. In addition, the big cells should be observed individually by microscopic analysis to determine the proportion that are dividing and returning to normal-sized leukemia cells (i.e. are clonogenic) versus the proportion that have been killed by sonication (i.e. are not clonogenic). With more refined observations of individual cells, we could determine what is causing the big cells to be depleted in number.

The cells from the CB-treated population showed a four-day delay in growth compared to the control cells. It appears, though, that they grew similarly to the control cells after that, both reaching a point of confluence, although the control cells reached that point roughly four days earlier than the CB-treated cells. Despite the shift in growth rate, the small cells seemed to behave like the control

cells that were never treated with CB. Whether they really do resemble control cells in other features is not known. Since the cycle time in 20% FBS medium is about 18 hours, a four-day difference in growth rate represents 5.3 doublings. This indicates an 80% difference in cell viability or a slower cell cycle time for the CB-treated enlarged, purified cells versus the control U937 leukemia cells.

Other characteristics of these CB-treated small cells would be of interest as well. For instance, do they resist becoming enlarged when treated with a second exposure to CB or do they represent a distinct sub-population of U937 cells with some innate feature that prevents them from enlarging and multinucleating? Even though the leukemia cells all come from the same U937 human promyleocytic cell line, stable sub-populations could exist that respond differently to CB. U937 leukemia forms several different types of differentiated hematopoietic cell clones in agarose that could arise from different cell sub-populations. Further experiments into the properties of these cells need to be performed in order to fully understand their differences.

One significant problem that was encountered in the experiment was mold contamination in a few tubes at the late stages of regrowth. If initial mold growth began as early as day 6 but did not become evident until day 9, the mold growth could affect results in certain tubes showing anomalous growth. Agarose cloning, by Dr. Thomas Fondy, of the 23 tubes showed mold growth in only two of the tubes, and this growth appeared 15 days after seeding, demonstrating that mold contamination on day 0 was not a problem. Contamination could have been introduced into some regrowth tubes during the process of multiple sampling on days 2, 4, 6, and 9. Without late stage mold contamination in some tubes, the experiment could have been followed for additional days. However, the key

observations had already been made by day 9, so late stage mold growth in some tubes was apparently only of minor consequence.

One major limitation of our experiment was that we performed the sonication with an ultrasonic bath cleaner designed to clean laboratory instruments. In future experiments, it would be best to use a more reliable source of ultrasound that has a power output that can be modulated and can provide consistent levels of acoustic cavitation. We calculated the power output of the ultrasound bath using Fourier's law of thermal conduction based on the temperature difference caused by the sonication and the amount of time sonicated (see Appendix E). Using a more precise instrument with a known power output and cavitation that can be varied would be costly, but it would make the results more reliable and allow us to investigate sonic effects at levels less than 0.77 watts that were employed in the current experiment. This would permit a test of longer sonication times without raising the temperature to the point where thermal effects directly destroy the cells. If the intensity of the ultrasound could be varied in a systematic way, it might also be possible to find the threshold intensity for immediate disruption of the large cells.

Overall, the data demonstrate some effects that correlate directly with the amount of sonication that was applied to the CB-treated U937 leukemia cells and that were not displayed in the control cells. Two examples are the statistically significant inhibited growth rate at days 2 and 6 as well as a difference in the non-sonicated versus sonicated CB-treated cells with respect to the percent of trypan blue dead cells. One way to definitively demonstrate an effect would be to look for a level of sonication that has a clear-cut effect on the controls and compare

that to effects on the CB-treated cells. It is hypothesized that if a strong enough amount of sonication is used for a long period of time, all cells would be killed.

If a differential effect of sonication on the CB-treated cells in comparison with non CB-treated leukemia cells can be confirmed, this could potentially introduce ultrasound as a physical modality in leukemia treatment. The sonication could be combined with other physical and chemical modalities to potentially enhance and increase the cytotoxic effects of microfilament agents in treatment in pre-clinical animal models. For example, we are proposing that sonication may have enhanced effects on enlarged CB-treated cells under hyperthermic conditions, in hypotonic medium, or if the cells are treated with microtubule-directed agents that may render the enlarged cells even more sensitive to sonic cavitation.

## REFERENCES

- Alberts, B., Bray, D., Hopkin, K., Johnson, A., Lewis, J., Raff, M., Roberts, K., & Walter, P. (2004). *Essential Cell Biology*. Spain: Garland Science.
- Brown, S. and Spudich, J. (1981). Mechanism of Action of Cytochalasin: Evidence that it Binds to Actin Filament Ends. *The Journal of Cell Biology*, 88, 487-491.
- Cochran, Stephen and Mark Prausnitz. (2001). Sonoluminescence as an Indicator of Cell Membrane Disruption by Acoustic Cavitation. *Ultrasound in Medicine & Biology*, 27, 841-850.
- Collins, K., Jacks, T., and Pavletich, N. (1997). The Cell Cycle and Cancer. *Proceedings of the National Academy of Sciences*, 94, 2776-2778.
- Cooper, Stephen. (2004). Control and Maintenance of Mammalian Cell Size. *BMC Cell Biology*, 5, article 35.
- Feril Jr., L. and Kondo, T. (2004). Biological Effects of Low Intensity Ultrasound: The Mechanism Involved, and its Implications on Therapy and on Biosafety of Ultrasound. *Journal of Radiation Research*, 45, 479-489.
- Flanagan, M. and Lin, S. (1980). Cytochalasins Block Actin Filament Elongation by Binding to High Affinity Sites Associated with F-actin. *The Journal of Biological Chemistry*, 255, 835-838.
- Law, D. and Reed, S. (1995). Cell Cycle Control of Morphogenesis in Budding Yeast. *Current opinion in Genetics and Development*, 5, 17-23.
- Lee, E., Gallagher R., Campbell A., and Prausnitz, M. (2004). Prediction of Ultrasound-Mediated Disruption of Cell Membranes Using Machine Learning Techniques and Statistical Analysis Applied of Acoustic Spectra. *IEEE Transactions on Biomedical Engineering*, 51, 82-89.
- Lin, S., Santi, D.V., and Spudich, J.A. (1973). Biochemical Studies on the Mode of Action of Cytochalasin B. Preparation of [3H] Cytochalasin B and Studies on its Binding to Cells. *The Journal of Biological Chemistry*, 249, 268-274.
- Liu, J., Lewis, T., and Prausnitz, M. (1998). Non-Invasive Assessment and Control of Ultrasound-Mediated Membrane Permeabilization. *Pharmaceutical Research*, 15, 918-924.
- McKinnell, R. (1998). Metastasis. In: R. McKinnell, R. Parchment, A. Perantoni,

and G. Pierce (eds.), *The biological basis of cancer*. pp. 50-78. USA:  
Cambridge University Press.

Nakaseko, Y. and Yanagida, M. (2001). Cytoskeleton in the Cell Cycle. *Nature*,  
412, 291-292.

## Appendix A

## Cell Viability form

## Appendix B

## Coulter Count form

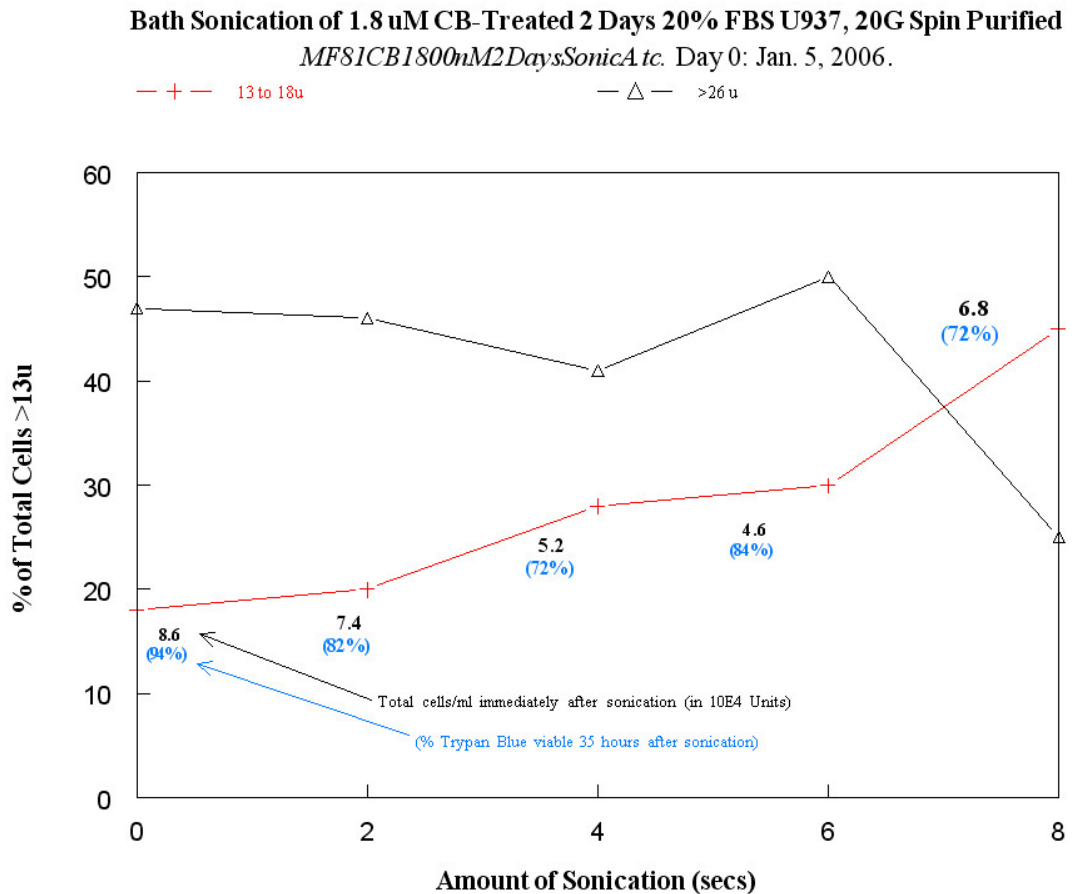
## Appendix C

Raw Data for the Sonication of the CB-Treated U937 Leukemia  
 Cells taken from 19  $\mu$  Steel Mesh Separation (1.25  $\mu$ M CB, 36 hours, 20%  
 FBS Medium)

Tube	Days after Sonication	# of Viable Big Cells	# of Viable Small Cells	# of Total Viable Cells	% Total Viable Big
0 secs	0	9	3	12	75
	2	18	41	59	32
	4	17	70	87	20
	6	7	125	132	6
	9	2	129	131	2
	11	0	89	89	0
2 secs	0	4	10	14	29
	2	23	31	54	47
	4	10	39	49	22
	6	17	94	111	16
	9	2	184	186	1
	11	0	88	88	0
4 secs	0	3	4	7	43
	2	12	31	43	26
	4	4	39	43	10
	6	6	66	72	9
	9	9	202	211	5
	11	----	----	----	----
6 secs	0	2	5	7	29
	2	4	10	14	31
	4	11	24	35	31
	6	4	50	54	6
	9	5	188	193	3
	11	0	63	63	0
8 secs	0	5	1	6	75
	2	3	15	18	17
	4	2	20	22	7
	6	5	52	57	9
	9	6	181	187	3
	11	0	95	95	0
10 secs	0	10	3	13	77
	2	5	27	32	15
	4	14	38	52	27
	6	12	128	140	9
	9	1	183	184	1
	11	----	----	----	----

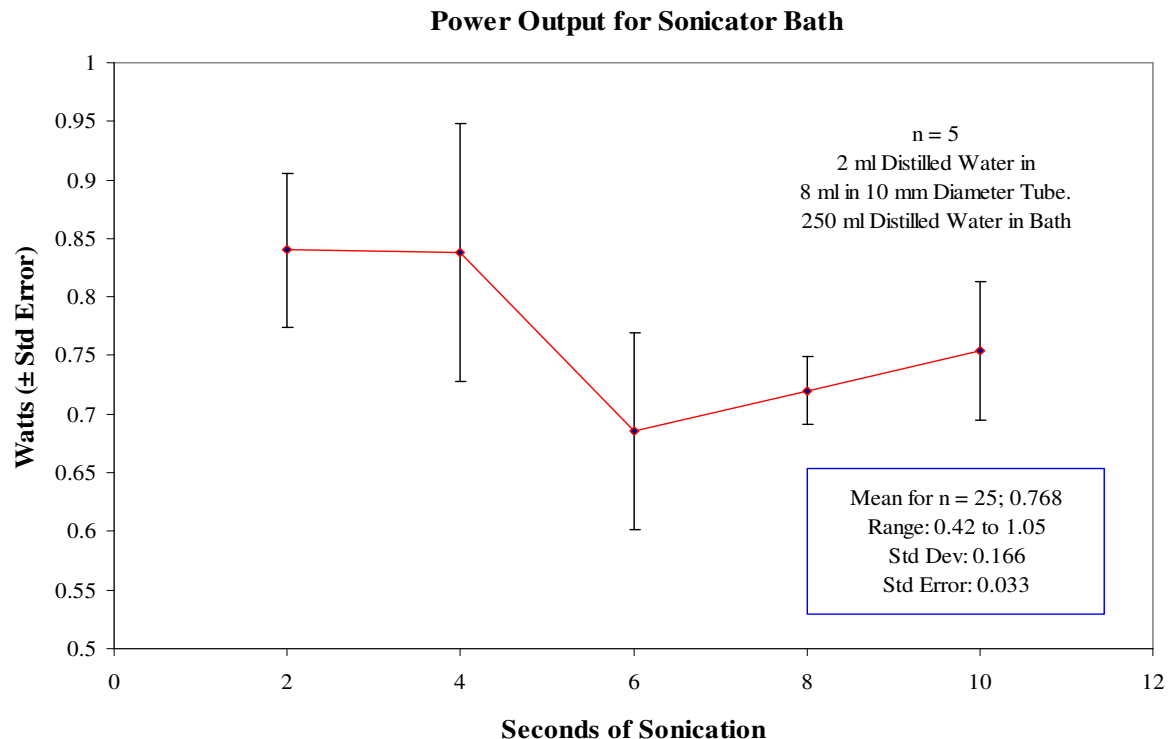
## Appendix D

### Distribution of cell sizes post-sonication



## Appendix E

### Power Output for Sonicator Bath



$$P = \frac{\rho V C_v \Delta T}{t}$$

P= Output power

$\rho$ =density of water = 1 g/ml

V=volume in test tube = 2 ml

$C_v$  = specific heat of the water at constant volume = 4.186 J/(g°C)

T=temperature difference

t = time sonicated